ELSEVIER

Journal of Materials Processing Technology 67 (1997) 207–213

Journal of Materials Processing Technology

Three-dimensional finite-element analysis of the compression molding of sheet molding compound

Soo-Young Kim, Yong-Taek Im *

Department of Mechanical Engineering, Korea Advanced Institute of Science & Technology, 373-1 Kusong-dong, Yusong-gu, Taejon 305-701, South Korea

Abstract

In order to analyze the compression molding of SMC (sheet molding compound) at room temperature, a three-dimensional finite-element program was developed based on the rigid–viscoplastic approach. The accuracy of the program developed was tested by solving the axi-symmetric compression of a cylindrical specimen of SMC and the three-dimensional compression of rectangular specimens of aluminum alloys under various processing conditions. The simulation results compared well with experimental results obtained from compression tests and with data available in the literature. Based on these comparisons the program was proven to be valid and was further applied in the simulation of the compression molding of rectangular SMC specimens to investigate the effect of friction and molding speeds on the propagation of the flow front of the material and the load requirements in the present investigation. By coupling part of the program with thermal analysis, the currently-developed analysis program can be utilized in determining detailed information during three-dimensional deformation processes. © 1997 Elsevier Science S.A.

Keywords: Finite-element analysis; Compression molding; Sheet molding compound

1. Introduction

In recent years, owing to improvement in manufacturing technology and reduction in production costs, the application of composite materials is increasing in various fields of industry. Amongst these composite materials, sheet molding compound (SMC) exhibits a combination of stiff and strong mechanical properties and good dimensional stability. In addition, SMC is easy to handle and its material and processing costs are relatively low. Thus, SMC has recently become a good candidate for replacing sheet metal parts in the automotive industry in an effort to produce light, stiff, strong and non-corrosive automotive outer panels.

SMC is a variety of polyester-based thermosetting molding material reinforced with randomly distributed short fiber glass strands. Using the compression-molding process, SMC can be manufactured easily. In a compression-molding cycle, the mechanics of the compression molding of SMC are influenced by the material characterization, heat transfer, curing, and the contact boundary conditions between the molds and the SMC charge. Thus, it is very difficult to predict the flow mechanism in the mold, the temperature distribution, the curing rate, and the distribution and orientation of the fiber glass strands.

Many studies have been carried out so far in determining the propagation of the flow front based on isothermal lubrication theory. Recently, Lee et al. [1] extended their work to include normal stresses and heat-transfer effects in their simulation. Also, a transverse viscosity gradient was added by Lee et al. [2] in simulating the formation of preferential flow. Experimental work done by Marker et al. [3] and Lee et al. [4] showed such preferential flow near to the mold surface when the SMC charge was compressed slowly. However, Barone and Caulk [5] reported that preferential flow occurred only in thick SMC charges molded at very slow closing speeds. Based on experimental findings and due to limitations of the existing analysis model, Lee et al. [6] tried to measure friction and investigated the effect of friction between the molds and the charge on the flow mechanism and the pressure

* Corresponding author. Fax: +82 42 8693210; e-mail: ytim@convex.kaist.ac.kr.

PII S0924-0136(96)02845-2

requirements during axi-symmetric and plane-strain molding using silly-putty [1] and an SMC charge without a curing agent. They assumed SMC to be a non-isothermal and viscoplastic material. According to their analysis, the numerically calculated pressure was still lower than the measured experimental data, such discrepancy being partly due to difficulty involved in the characterization of the material.

In order to develop a three-dimensional finite-element program for the analysis of the compression molding of SMC, the non-isothermal deformation was divided into two parts, the first being a deformation part and the second a temperature analysis, including curing analysis. As a first step in the development stage, a three-dimensional viscoplastic deformation program was completed, the program developed being tested by solving the axi-symmetric compression of a cylindrical specimen of SMC under various processing conditions, then being further applied in solving the compression molding of SMC at room temperature with two friction conditions and molding speeds, to investigate the effect of these values on the flow of the material.

2. Finite-element formulation

Since detailed information about the finite-element formulation for rigid–viscoplastic deformation analysis is available elsewhere [7], only the highlights of the formulation will be described here. The governing equations for the solution of the mechanics of the plastic deformation of rigid-viscoplastic materials are summarized in tensorial notation as follows:

Equilibrium equations:

$$\sigma_{ij,j} = 0. \tag{1}$$

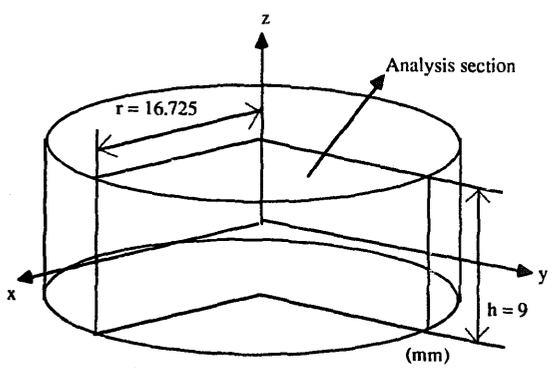

Fig. 1. Initial cylindrical specimens used in the compression simulations.

[1] Silly-putty is a viscoelastic polymer and exhibits a flow behavior with strong temperature dependence.

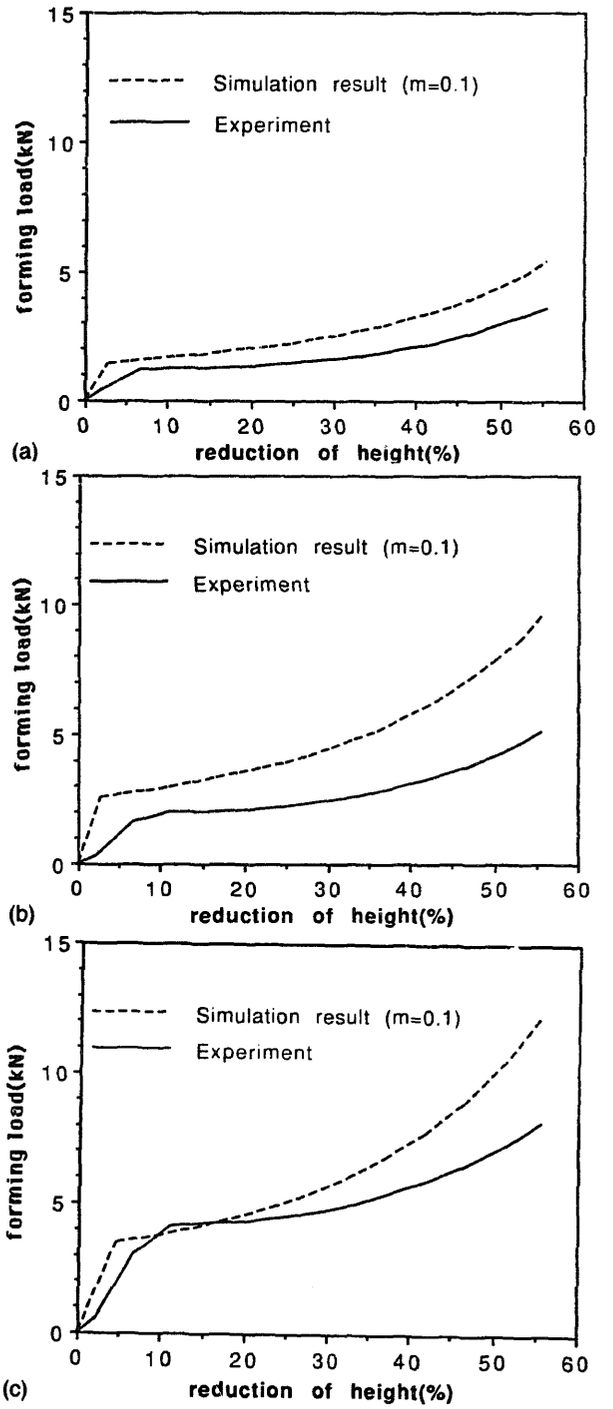

Fig. 2. Comparisons of compression loads between simulation and experiment at various mold closing speeds: (a) $v = 10$ mm min^{-1}; (b) $v = 30$ mm min^{-1}; and (c) $v = 50$ mm min^{-1}.

Boundary conditions:

$$u_i = u_i^* \text{ on } S_U, \quad \text{and} \quad t_i = t_i^* \text{ on } S_F. \tag{2}$$

Yield criterion:

$$f(\sigma_{ij}) = 0, \qquad \bar{\sigma} = \sqrt{\tfrac{3}{2}(\sigma'_{ij}\sigma'_{ij})} = \bar{\sigma}(\bar{\varepsilon}, \dot{\bar{\varepsilon}}). \tag{3}$$

Constitutive equations:

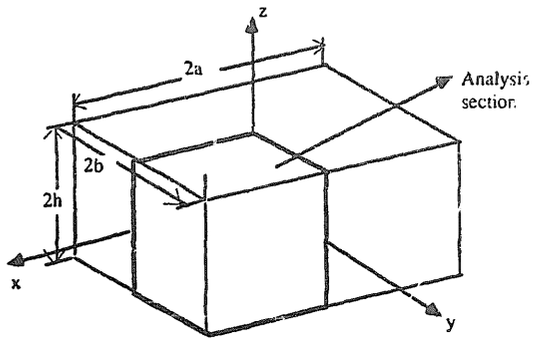

Fig. 3. Initial workpiece geometry used in the block compression of aluminum alloys.

$$\dot{\varepsilon}_{ij}=\frac{\partial f(\sigma_{ji})}{\partial \sigma_{ij}}\dot{\lambda}, \qquad \dot{\varepsilon}_{ij}=\frac{3\,\dot{\bar{\varepsilon}}}{2\bar{\sigma}}\sigma'_{ij}, \quad \text{and} \quad \dot{\bar{\varepsilon}}=\sqrt{\tfrac{2}{3}(\dot{\varepsilon}_{ij}\,\dot{\varepsilon}_{ij})}. \tag{4}$$

Compatibility conditions:

$$\dot{\varepsilon}_{ij}=\tfrac{1}{2}(u_{i,j}+u_{j,i}). \tag{5}$$

Here, σ'_{ij} represents the deviatoric stress tensor. By applying the weak form to the equilibrium equation and the divergence theorem under the assumption of no body and inertia forces, the following equation can be obtained:

$$\int_V (\tfrac{2}{3}\bar{\sigma}/\dot{\bar{\varepsilon}}\dot{\varepsilon}_{ij})\delta\dot{\varepsilon}_{ij}\,\mathrm{d}V-\int_{S_F} t_i^*\delta v_i\,\mathrm{d}S+\int_V K\dot{\varepsilon}_{kk}\delta\dot{\varepsilon}_{ii}\,\mathrm{d}V=0. \tag{6}$$

Here, K represents a penalty constant. By introducing the eight-node brick element, this equation can be discretized as follows:

$$\int_V (\bar{\sigma}/\dot{\bar{\varepsilon}})\mathbf{B}\mathbf{D}^{\mathrm{T}}\mathbf{B}^{\mathrm{T}}\mathbf{v}\,\mathrm{d}V+\int_V K\mathbf{B}\mathbf{c}^{\mathrm{T}}\mathbf{c}\mathbf{B}^{\mathrm{T}}\mathbf{v}\,\mathrm{d}V-\int_{S_F}\mathbf{N}^{\mathrm{T}}\mathbf{t}\,\mathrm{d}S=0. \tag{7}$$

Here, N and v matrices represent the shape function and the nodal velocity, respectively. The detailed component form of the B, c and D matrices can be determined easily or found in Ref. [7]. The friction force between the dies and charge was modeled by the following equation as a traction term:

$$t=m_f\frac{\bar{\sigma}}{\sqrt{3}}\left(\frac{2}{\pi}\tan^{-1}\left(\frac{|v_r|}{a}\right)\right)\frac{v_r}{|v_r|}. \tag{8}$$

Table 1
Initial workpiece dimensions in mm and friction values (m_f) used in block compression simulations

Simulation No.	2a	2b	a/b	2h	m_f
1	19.05	19.05	1	9.525	0.1 (lub.)
2	19.05	19.05	1	9.525	0.5 (dry)
3	38.10	19.05	2	9.525	0.2 (lub.)
4	38.10	19.05	2	9.525	0.5 (dry)

Table 2
Comparisons of deformed length at the x and y axes for various block compression cases (all values in mm) between simulations and experiments available in [8]

Simulation No.	Experiment [8] (50% reduction)		Simulation (52.5% reduction)	
	a	b	a	b
1	13.5	13.5	13.98293	13.98293
2	14.1	14.1	14.57700	14.57700
3	15.0	24.5	15.51393	25.19647
4	16.6	24.2	16.13536	23.99101

Here, a (= 0.05) is a small positive number compared to v_r, which represents the sliding velocity of a charge relative to the mold closing speed, and m_f represents the constant shear friction factor between the dies and the charge. Considering the non-linearity of the problem, the discretized governing equation should be linearized and solved using the Newton–Raphson method. Based on these equations, the three-dimensional finite-element program was developed.

3. Numerical results and discussion

3.1. Axi-symmetric analysis of the compression test of cylindrical SMC charges

Using the flow stress obtained by a compression test in the laboratory using grease oil as a lubricant, the axi-symmetric SMC compression molding of a cylindrical charge was simulated. The mold closing speeds used in the simulations were 10, 30, and 50 mm min^{-1}, and the friction factors were assumed to be $m_f=0.1$ and 0.01. The diameter and height of the cylinder were 33.4 and 9 mm, respectively. The geometry of the charge used in the simulations was the same for all of the compression tests that were carried out in the experiments. Only one quarter section, as shown in Fig. 1, was used for simulations due to the symmetry of the problem. The following flow stress equation obtained from compression tests with grease and mylar sheet between the dies and the SMC charge was used in the present investigation:

$$\sigma=C(T)\dot{\bar{\varepsilon}}^{m(T)},$$

$$C(T)=4.5083\times10^{-5}\exp\left(\frac{3732.2}{T}\right),$$

$$m(T)=2.31634\exp\left(\frac{-447.37}{T}\right). \tag{9}$$

Here, the stress is given in MN m^{-2}, and T is absolute temperature.

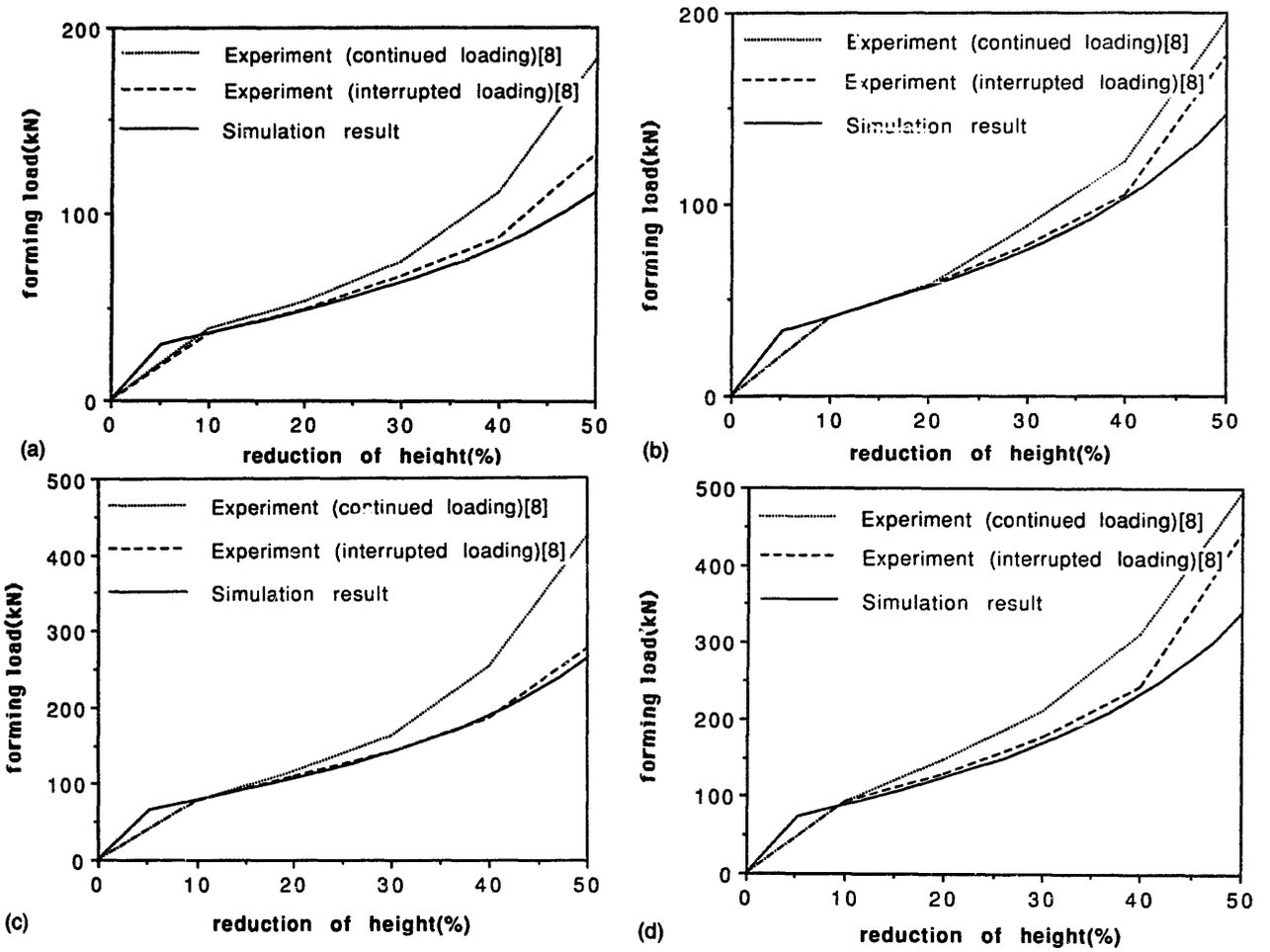

Fig. 4. Comparisons of forging loads between simulation and experiment in [8] for various loading conditions: (a) $a/b = 1$, $m_f = 0.1$; (b) $a/b = 1$, $m_f = 0.5$; (c) $a/b = 2$, $m_f = 0.2$; and (d) $a/b = 2$, $m_f = 0.5$.

In Fig. 2, load–stroke curves obtained by experiment and simulation are compared to each other. It can be seen from these figures that the predicted values were reasonably accurate for the compression molding conditions of both mold closing speeds of 10 mm min^{-1} and 50 mm min^{-1}, but they were considerably greater for the case of a mold closing speed of 30 mm min^{-1}. In general, the simulation results were higher compared to the measured data. This kind of over-prediction was due to difficulty in determining the rheological characteristics of the SMC material because of the incorporation of glass fibers as a reinforcement. Accounting for this factor, the accuracy of the program developed was acceptable, but more accurate simulation results would be obtained should more appropriate rheological data be available.

3.2. Analysis of the compression of rectangular specimens of aluminum alloys

In Fig. 3 the geometry of the initial rectangular specimen is depicted. The various simulation cases are summarized in Table 1. Because of the symmetry of the geometry, only one quarter section was used in the simulations. For the material property data, the following data available in the literature [8] was used:

$$\bar{\sigma} = 62.74(1.0 + \bar{\varepsilon}/0.05205)^{0.3} \ (\mathrm{MN\,m^{-2}}). \tag{10}$$

Comparisons between the computed and tested data in [8] are given in Table 2. It can be seen from this table the computed data was reasonably accurate, the errors between the two being $0.9 \sim 3.6\%$.

In Fig. 4, the forming loads were compared for two different loading conditions: continuous and interrupted. From these figures, the predictions were more accurate for the interrupted cases, as reported in [8]. This was due partly to the change of the friction conditions according to deformation levels in the continuous loading cases, compared to the interrupted cases where the lubrication was updated when the deformation was interrupted.

From these two numerical simulations, it was construed that the developed three-dimensional program was reasonably accurate in analyzing three-dimensional deformation at room temperature.

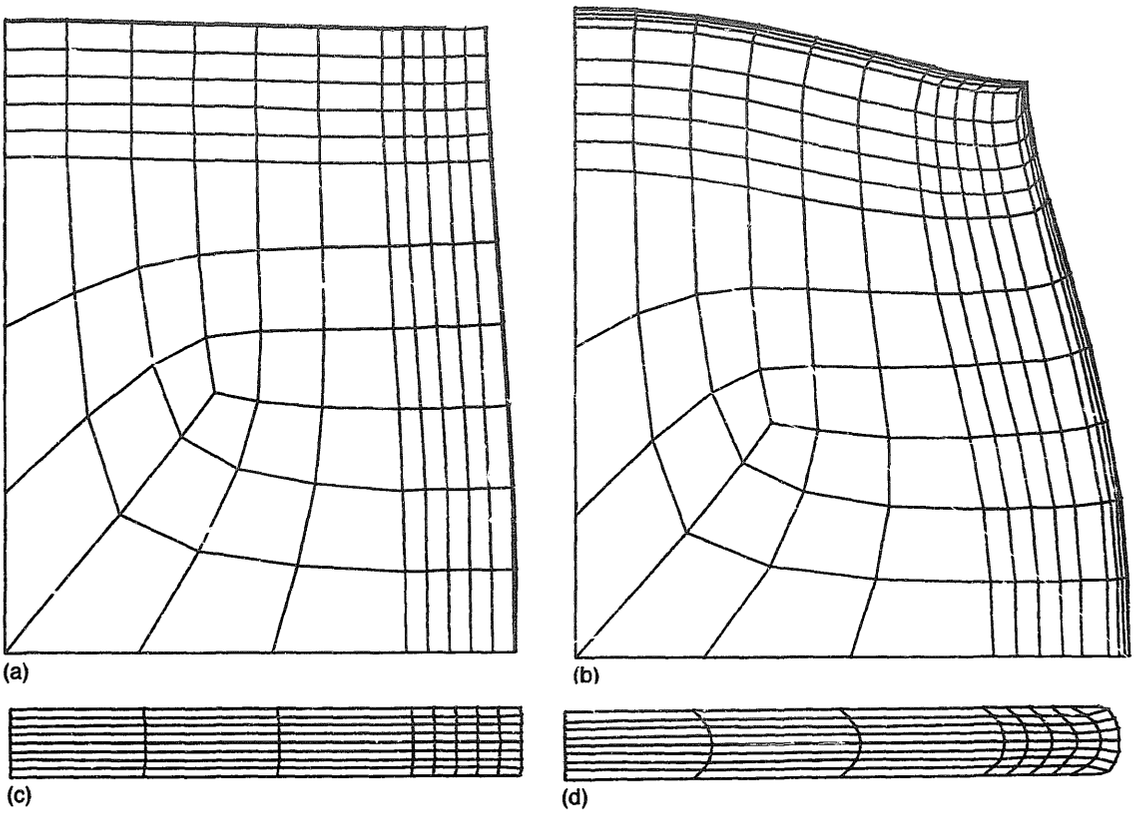

Fig. 5. Comparisons of the deformed shapes of compressed rectangular SMC specimens at 38.2% reduction of height at the x–y and x–z planes with different friction conditions: (a) $v = 15$ mm min^{-1}, $m_f = 0.1$ (in the x–y plane); (b) $v = 15$ mm min^{-1}, $m_f = 0.8$ (in the x–y plane); (c) $v = 15$ mm min^{-1}, $m_f = 0.1$ (in the x–z plane); and (d) $v = 15$ mm min^{-1}, $m_f = 0.8$ (in the x–z plane).

3.3. Analysis of the SMC compression molding of rectangular charges

To investigate the effect of friction and compression speed on the deformation of SMC at room temperature during molding, the compression molding simulation of a rectangular charge was carried out under two friction ($m_f = 0.1$ and 0.8) and velocity ($v = 15$ and 45 mm min^{-1}) conditions. Because of the symmetry of the geometry, only one quarter section was used in the simulations. The initial dimension of the SMC block was $76.7 \times 101 \times 11$ (mm^3). 898 brick elements and 1188 nodal points being used for simulations. The material property used for the simulations was selected from Ref. [9], as follows:

$$\bar{\sigma} = C(T)\dot{\bar{\varepsilon}}^{m(T)},$$

$$C(T) = 8.123 \times 10^{-4} \exp\left(\frac{2182.3}{T}\right),$$

$$m(T) = 1.45 - 2.52 \times 10^{-9} \exp\left(\frac{5775.8}{T}\right). \quad (11)$$

Here, the dimension is given in kgf mm^{-2} (1 kgf mm^{-2} = 9.81 MPa) and T is in absolute temperature. It can be found from the comparison of Eqs. (9) and (11) that the material property data is different from that of each other because of difference in the batches and in curve fitting. Therefore, it is very important to determine the proper material data in order to obtain reasonable simulation results, as mentioned earlier.

Deformed shapes in the x–y and x–z planes at 38.2% reduction of height with a mold closing speed of 15 mm min^{-1} under two different friction conditions are shown in Fig. 5. From this figure, it was found that as friction increased, the bulging increased. The simulation results are not shown here, since the deformed shape was almost similar to Fig. 5 in the case of a mold closing speed of 45 mm min^{-1}. However, if the order of the closing speed is increased, the flow front becomes flat, like plug flow.

The effective strain and its rate distributions at 38.2% reduction of height for various cases are given in Figs. 6 and 7, respectively. These figures show that the distribution patterns are similar in general, with the maximum values of effective strain and its rate increasing as the closing mold speed and friction increase. From this observation, it was construed that the effect of friction on the deformation levels was more significant than that of the closing speed, under the present molding conditions.

The forming load increased as closing speed increased as shown in Fig. 8. From this figure, it can be

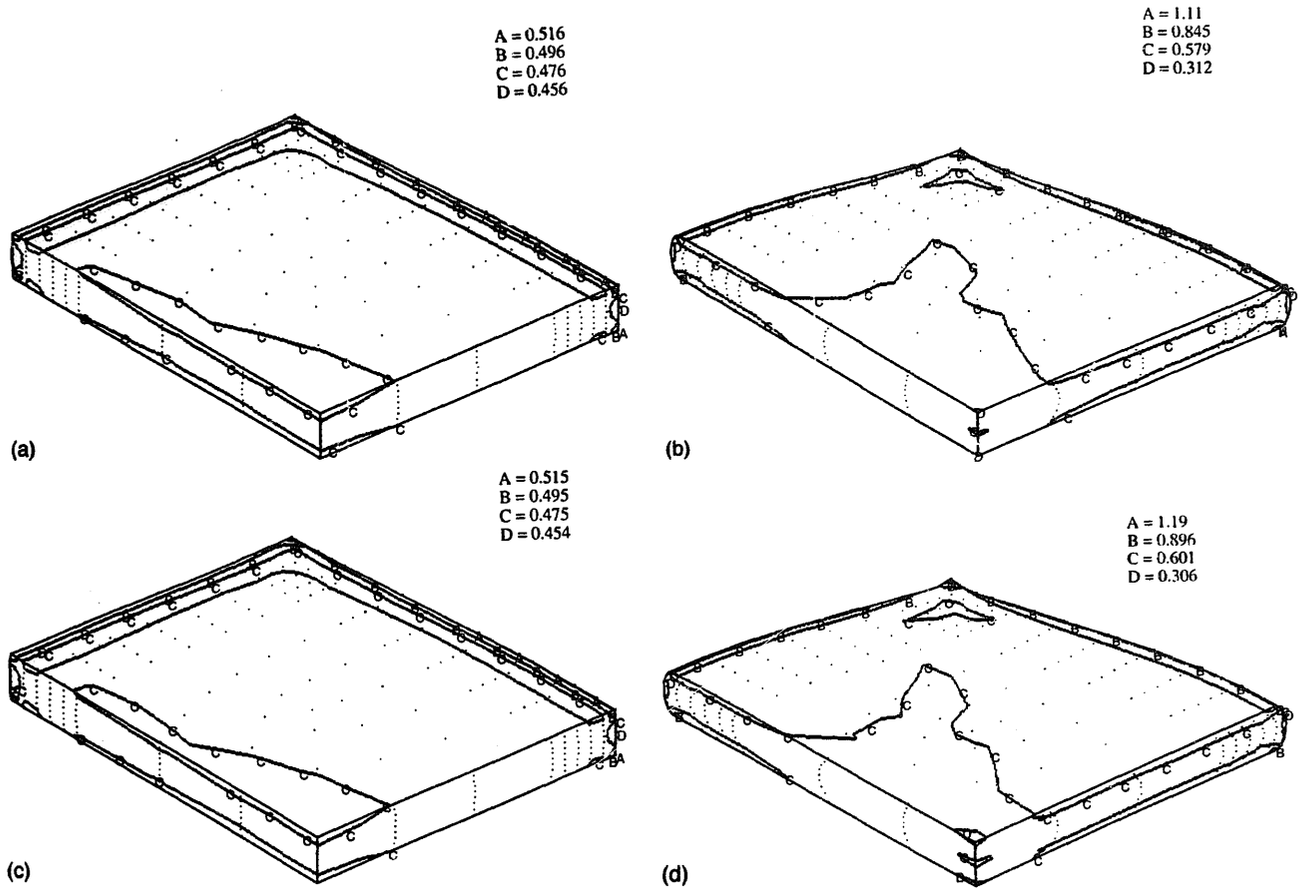

Fig. 6. Effective strain distributions of compressed rectangular SMC specimens at 38.2% reduction of height for various cases: (a) $v = 15$ mm min^{-1}, $m_f = 0.1$; (b) $v = 15$ mm min^{-1}, $m_f = 0.8$; (c) $v = 45$ mm min^{-1}, $m_f = 0.1$; and (d) $v = 45$ mm min^{-1}, $m_f = 0.8$.

seen that both the effect due to friction and that due to closing speed play a significant role in influencing the forming loads.

4. Conclusions

In the present investigation a three-dimensional finite-element program was developed successfully. From comparison of simulation results with experimental data in terms of forming load and geometry changes, the accuracy of the program developed was reasonable under the present molding conditions. It was found that the friction effect is more significant in determining flow patterns during compression molding at room temperature, and also found that both the effects due to friction and those due to closing speed are noticeable with increasing deformation and level of forming load.

Since the compression molding process is non-isothermal, a temperature analysis program, including the curing reaction, should be developed and coupled into the next stage of investigation to complete the analysis. Once the coupled analysis program is available it will be very useful for investigating the effect of the molding parameters and rheological properties on the flow of the material and its mechanical properties.

Acknowledgements

The authors express their thanks to KOSEF and the Cray Research, Inc. for the grant under which this work was more possible, and to LG Chemical Co. for providing the SMC materials.

References

[1] C.C. Lee and C.L. Tucker, Flow and heat transfer in compression mold filling, *J. Non-Newtonian Fluid Mech.*, *24* (1987) 245–264.

[2] S.J. Lee, M.M. Denn, M.J. Crochet and A.B. Metzner, Compressive flow between parallel disks, *J. Non-Newtonian Fluid Mech.*, *10* (1982) 3–10.

[3] L.F. Marker and B. Ford, Flow and curing behavior of SMC during molding, *Modern Plast.*, *54* (1977) 64–70.

[4] L.J. Lee, L.F. Marker and R.M. Griffith, The rheology and mold flow of polyester sheet molding compounds, *Polym. Compds.*, *2* (1981) 209–218.

[5] M.R. Barone and D.A. Caulk, Kinematics of flow in SMC, *Polym. Compds.*, *6* (1985) 105–109.

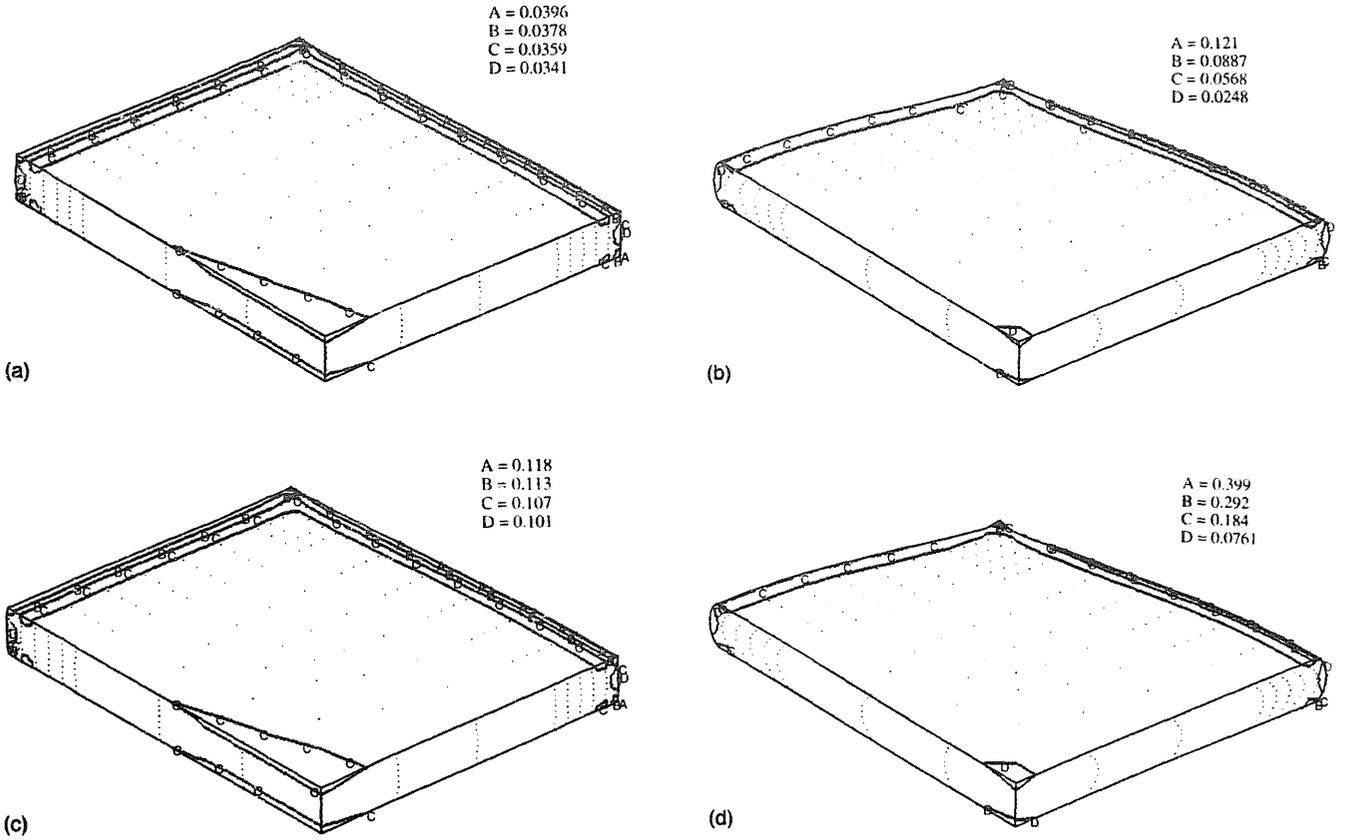

Fig. 7. Effective strain-rate distributions of compressed rectangular SMC specimens at 38.2% reduction of height for various cases. (a) $v = 15$ mm min^{-1}, $m_f = 0.1$; (b) $v = 15$ mm min^{-1}, $m_f = 0.8$; (c) $v = 45$ mm min^{-1}, $m_f = 0.1$; and (d) $v = 45$ mm min^{-1}, $m_f = 0.8$.

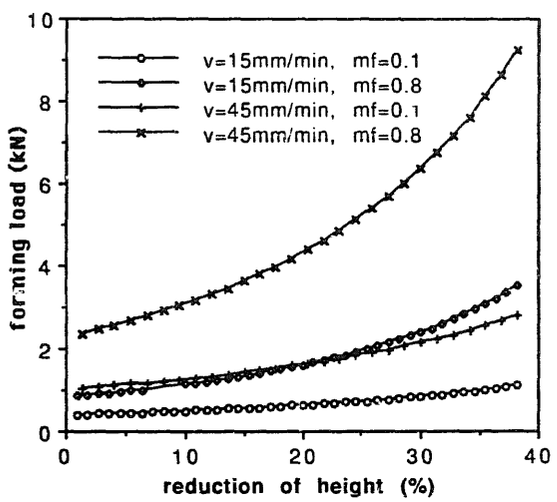

Fig. 8. Comparison of forming loads between simulations for various cases.

[6] L.J. Lee, G.D. Fan, J. Kim and Y.T. Im, Flow analysis of sheet molding compounds in compression molding, *Int. Polym. Process.*, *6* (1991) 61–72.

[7] S. Kobayashi, S.I. Oh and T. Altan, *Metal Forming and the Finite-Element method*, Oxford University Press, New York, 1989.

[8] J.J. Park and S Kobayashi, Three-dimensional finite element analysis of block compression, *Int. J. Mech. Sci.*, *26* (1984) 165–176.

[9] J.H. Cho and N.S. Kim, Analytical study of compression molding of SMC, *Proc. Spring Conf., KSME, Pusan, Korea, 1993*, pp. 256–261.